

Electronic Supplementary Information

**Stable Perovskite Solar Cells with 25.17% Efficiency Enabled by Improving
Crystallization and Passivating Defect Synergistically**

Yihui Wu ^{ab}, Qi Wang ^a, Yuting Chen ^a, Wuke Qiu ^a, and Qiang Peng ^{*ab}

^a School of Chemical Engineering and State Key Laboratory of Polymer Materials Engineering,
Sichuan University, Chengdu 610065, China.

E-mail: qiangpeng@scu.edu.cn

^b Engineering Research Center of Alternative Energy Materials & Devices, Ministry of Education,
Sichuan University, Chengdu 610065, China

1. Materials

All the chemicals were used as received. Lead iodide ($\geq 98\%$) was purchased from TCI. $\text{SnCl}_2 \cdot 2\text{H}_2\text{O}$ ($>99.99\%$) and anisole was purchased from Aladdin. Thioglycolic acid (TGA, 98%), urea, lithium bis(trifluoromethanesulfonyl)imide salt (Li-TFSI), and 4-tert-butylpyridine (tBP) were purchased from Sigma-Aldrich. Cobalt(III) tris(bis(trifluoromethylsulfonyl)imide) salt (Co(III) TFSI, FK209) were purchased from Greatcell solar. Formamidinium iodide (FAI), methylammonium chloride (MACl), methylammonium bromide (MABr), PbBr_2 , and spiro-OMeTAD were purchased from Xi'an p-oled Co., Ltd. 2-Amidinopyrimidine hydrochloride (APC, $>98\%$) was purchased from Adamas-beta. HCl aqueous (37 wt%) was purchased from CHRON Chemicals. Distilled water was purchased from Watsons. Dimethylformamide (DMF), dimethyl sulfoxide (DMSO), chlorobenzene (CB), isopropyl alcohol (IPA) and acetonitrile were purchased from Sigma-Aldrich and used without purification.

2. Device fabrication

All devices were prepared on the cleaned and patterned FTO substrates (AGC22-8A, purchased from Advanced Election Technology Co., Ltd.). The compact SnO_2 layer was fabricated using a chemical bath deposition (CBD) method. Briefly, 625 mg of urea and 137.5 mg of $\text{SnCl}_2 \cdot 2\text{H}_2\text{O}$ were dissolved in 50 mL of distilled water (purchased from Watsons). Then, 625 μL of HCl and 12.5 μL of TGA were added into this solution. The obtained CBD solution was loaded onto a glass reaction vessel (size: 65 mm * 61 mm * 92 mm, volume: ~ 140 mL, purchased from Taobao). The cleaned FTO substrate (8 small pieces) were vertically placed into the glass vessel and the reaction was kept at 90 °C (oil bath) for 5.5 h. After the reaction was complete, the SnO_2 deposited FTO substrate was removed from the reaction vessel and cleaned *via* sonication with distilled water and IPA for 5 min each. The FTO/ SnO_2 substrate was then annealed in an ambient environment at 170 °C for 60 min, followed by spin-coating 10 mM KCl in deionized water at 3000 rpm for 30 s and annealing at 100 °C for 10 min. Before perovskite deposition, the FTO/ SnO_2 substrate was treated by a UV-Ozone for 15 min.

The FAMA perovskite solution was prepared by mixing 1.53 M PbI_2 , 1.4 M FAI, 0.5 M MACl, and 0.0122 M MAPbBr_3 in DMF:DMSO (8:1, v/v). The perovskite solution deposited *via* spin coating at 1000 rpm for 10 s (200 rpm ramp) and 5000 rpm for 30 s (2000 rpm ramp). During 10 seconds into the second step, 110 μL of a mixed antisolvent (anisole: IPA = 9:1, v/v) was deposited

onto the substrate. For the APC containing samples (APC was dissolved in the mixed anti-solvent), the concentration of APC was tuned in the range of 0-0.1 mg/mL. And then, the wet film was annealed at 110 °C for 60 min. After the perovskite film was cooled down to room temperature, a 5 mg/mL of PEAI/IPA solution was spin-coated at 5000 rpm for 30 s and no annealing was required. After that, a solution of spiro-OMeTAD/CB (100 mg mL⁻¹) was spin-coated onto perovskite films at 4000 rpm for 30 s in glove box, where 40 μL 4-tert-butylpyridine, 24.5 μL Li-TFSI/acetonitrile (520 mg mL⁻¹), and 49 μL Co-TFSI/acetonitrile (300 mg mL⁻¹) were used as the additive. Finally, 8 nm of MoO₃ and 120 nm of Ag electrode were deposited by thermal evaporation.

For the MA-free, Cs/FA perovskite, the precursor solution is comprised of 52 mg of CsI, 186 mg of FAI, 8 mg of FABr, 591 mg of PbI₂, 18.6 mg of PbCl₂ in 1 mL of DMF and DMSO (4:1, v/v). The precursor solution was deposited on compact SnO₂ substrates by a consecutive two-step spin-coating process at 1000 and 4000 rpm for 10 and 40 s, respectively. 110 μL of mixed anti-solvent (anisole: IPA = 9:1, v/v) without or with 0.01 mg/mL APC was dropped onto the substrate at 20 s before the end. And then the wet film was annealed at 110 °C for 20 min. The fabrication procedures of PEAI, HTL and metal electrode are the same with that of the FAMA-based PSCs. After deposition of metal electrode, all devices were stored in a desiccator overnight and then the *J-V* curves were measured.

3. Characterization

The top-view and the cross-sectional SEM images were obtained by using a Titachi S4800 field-emission scanning electron microscopy (Hitachi High Technologies Corporation). AFM was recorded from Bruker Innova atomic microscopy. The UV-visible absorption spectra of the solution and thin films were measured from the absorbance model (without integrating sphere) using PerkinElmer Lambda 950 UV-vis spectrophotometer with a scanning rate of 600 nm/min in the range of 900-300 nm at a step bandwidth of 1 nm. The XRD patterns of the perovskite films were recorded on Bruker D8 advance with a Cu K α radiation (40 kV, 40 mA) and a scanning rate of 5°/min in the 2 θ range of 5-60° at a step size of 0.02 s. The steady PL spectra and time-resolved PL decay measurements were performed using an FLS980 Series of Fluorescence Spectrometers. For the PL measurement, the excitation source was a monochromatized Xe lamp (450W, Ozone free Xenon Arc Lamp, peak wavelength at 500 nm with a line width of 2 nm). For TRPL, the

excitation source was a supercontinuum pulsed laser sources (YSL SC-PRO) with an excitation wavelength at 800 nm, a repetition rate of 0.1 MHz, and a laser intensity of 10 mW/cm². Monochromatic external quantum efficiency (EQE) spectra were recorded as functions of wavelength with a monochromatic incident light of 1 x 10¹⁶ photons cm⁻² in alternating current mode with a bias voltage of 0 V (QE-R3011). The light intensity of the solar simulator was calibrated by a standard silicon solar cell provided by PV Measurements. Electrochemical impedance spectroscopy (EIS) was obtained by using a multi-channel potentiostat (VMP3, Biologic) under dark conditions in the frequency range from 1 MHz to 100 mHz with an AC amplitude of 30 mV. Mott-Schottky analysis was conducted by using a multi-channel potentiometer (VMP3, Biologic) at the frequency of 50 KHz in the applied voltage range from 0 V to 1.5 V with an AC amplitude of 25 mV. A Fourier transform infrared spectroscopy (FT-IR, Thermo Fisher Nicolet Is5) was used to collect the FT-IR spectral data for the samples without and with APC. The liquid state ¹H nuclear magnetic resonance (NMR) measurements were recorded on JNM-ECZ400S/L1 spectrometer (TMS as an internal standard ($\delta = 0$)). UPS and XPS spectra were recorded by a Thermo-Fisher ESCALAB Xi+ system. For XPS measurement, radiation was produced by a monochromatic 75 W Al K α excitation centred at 1486.7 eV. For UPS measurement, He I ultraviolet radiation source of 21.22 eV was used. The depth profile of the perovskite film on the ITO substrate was recorded using ToF-SIMS (model ION ToF-SIMS 5) with positive polarity. The pulsed primary Bi⁺ ion source was operated at 30 keV and 1 pA on a 100*100 μm^2 area to bombard the sample surface to produce secondary ions. The sputtering was performed with a O₂ ion beam operated at 1 keV and 100 nA on a 300*300 μm^2 area. The current-voltage characteristics were measured by Keithley 2400 source and the solar simulator with standard AM 1.5G (100 mW/cm², SAN EI: Japan) under ambient conditions. The *J-V* curves were measured by forward (-0.1 V to 1.5 V forward bias) or reverse (1.5 V to -0.1 V) scans with a delay time of 100 ms for each point. The *J-V* curves for all devices were obtained by masking the cells with a metal mask with area of 0.09 cm² or 1 cm². The devices for long-term stability measurement were stored in a N₂-filled glovebox. After various periods of time, the *J-V* measurements were performed. For the MPP measurement, to evaluate the influence of APC on the stability of perovskite, a Li-salt-free Spiro-OMeTAD was adopted to assemble the control and APC-treated devices. The dynamic MPP tracking was carried out in a home-made N₂-filled box under 1 sun

continuous illumination (white light LED array) with temperature of ~ 30 °C. The MPP was automatically recalculated every 2 h by tracking the J - V curve.

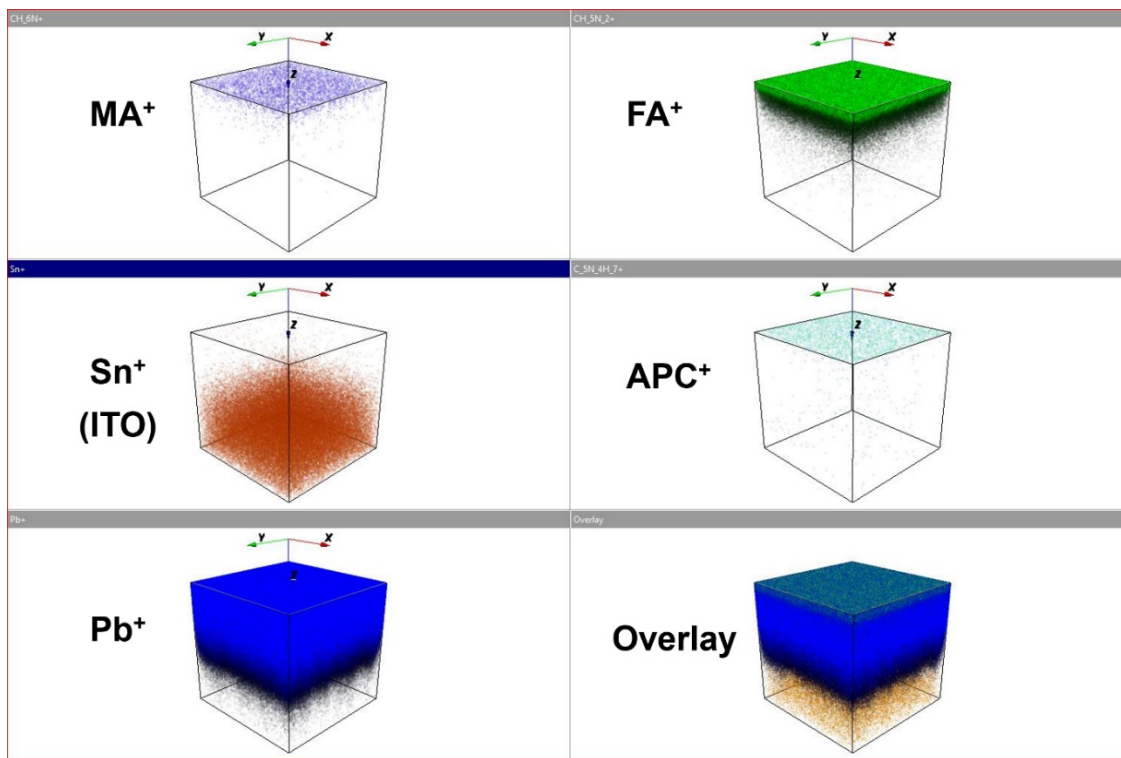


Fig. S1. Reconstructed elemental 3D maps of positive ions traced in the depth profile for APC treated perovskite films.

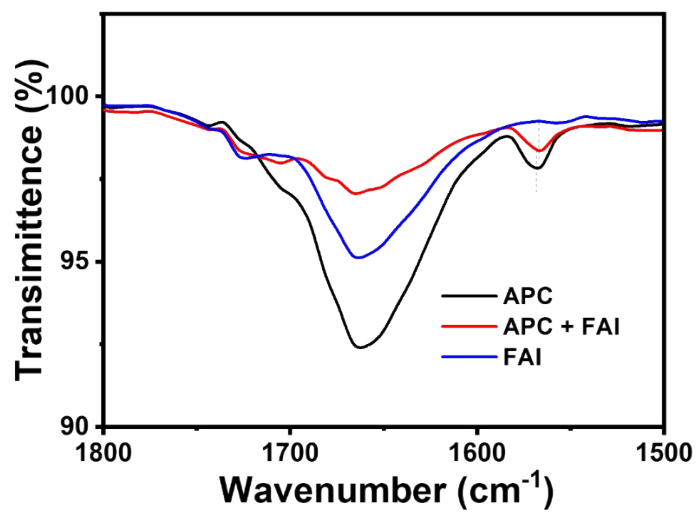


Fig. S2. FT-IR spectra of APC, FAI, and APC mixed FAI samples.

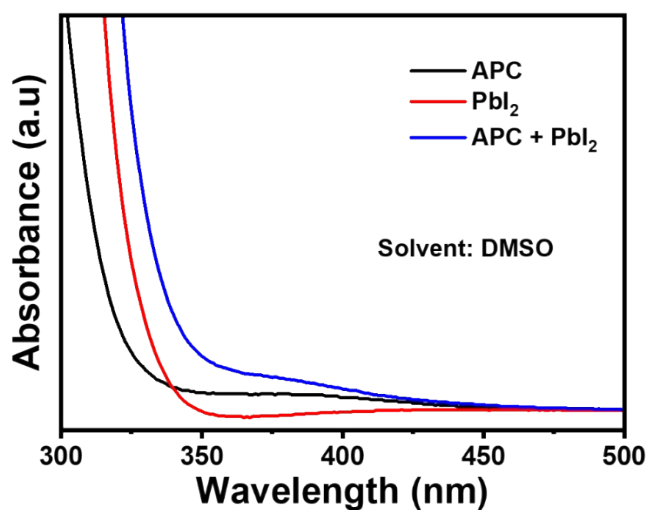


Fig. S3. UV-Vis absorption spectra of APC, PbI_2 , and APC mixed PbI_2 .

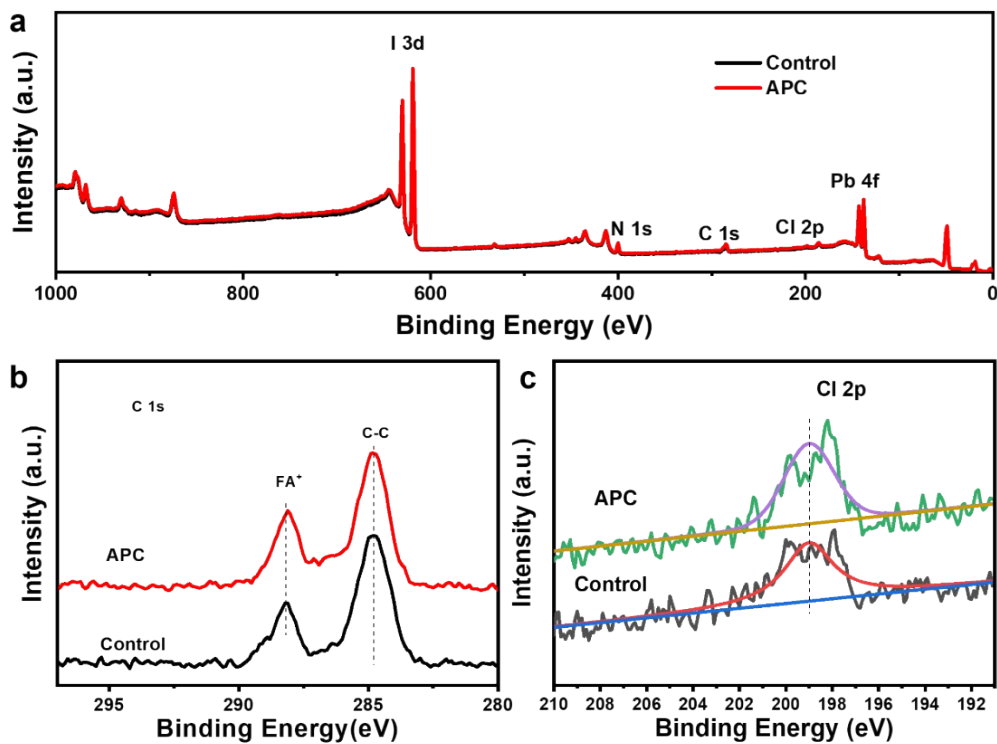


Fig. S4. XPS spectra of the control and APC treated perovskite films: (a) survey, (b) high resolution spectra of C 1s, and (c) high resolution spectra of Cl 2p.

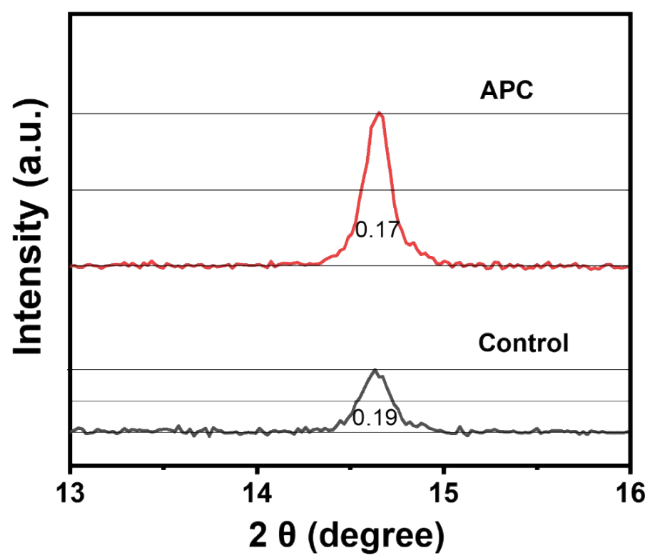


Fig. S5. Partially enlarged XRD patterns of the control and APC treated perovskite films.

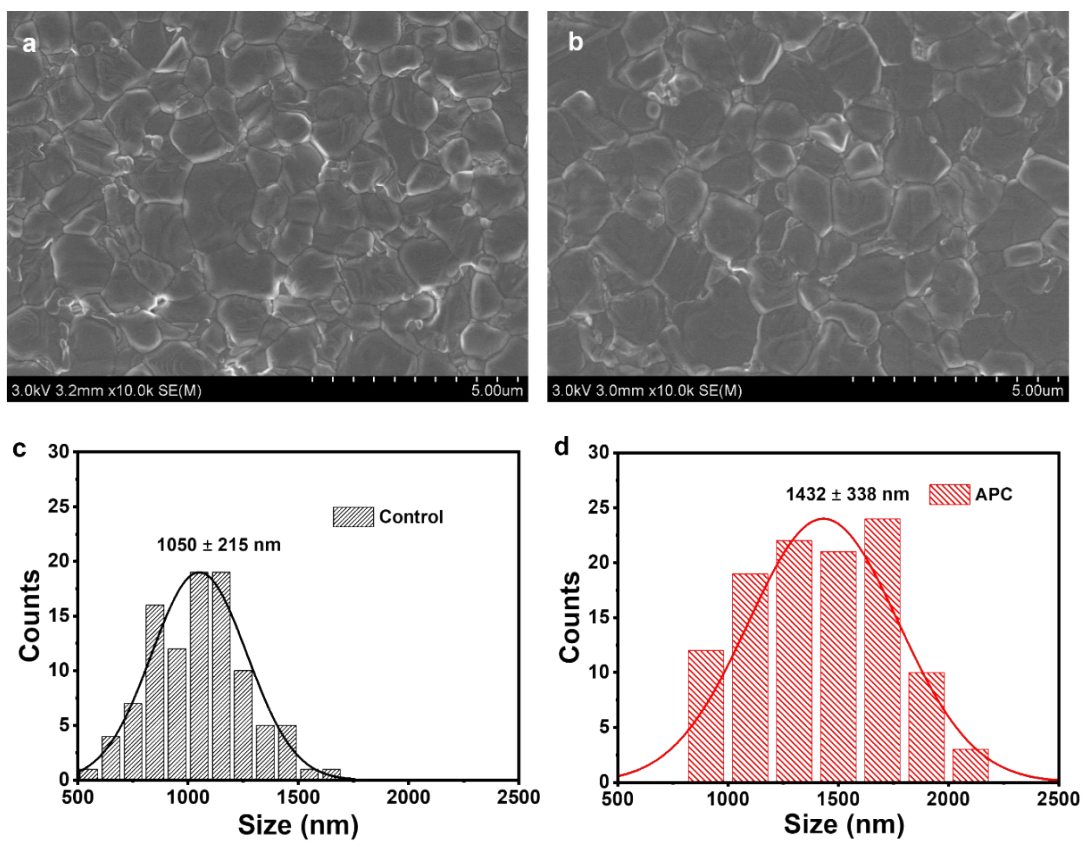


Fig. S6. SEM images and the corresponding grain size distributions of the control (a, c) and APC treated perovskite films (b, d).

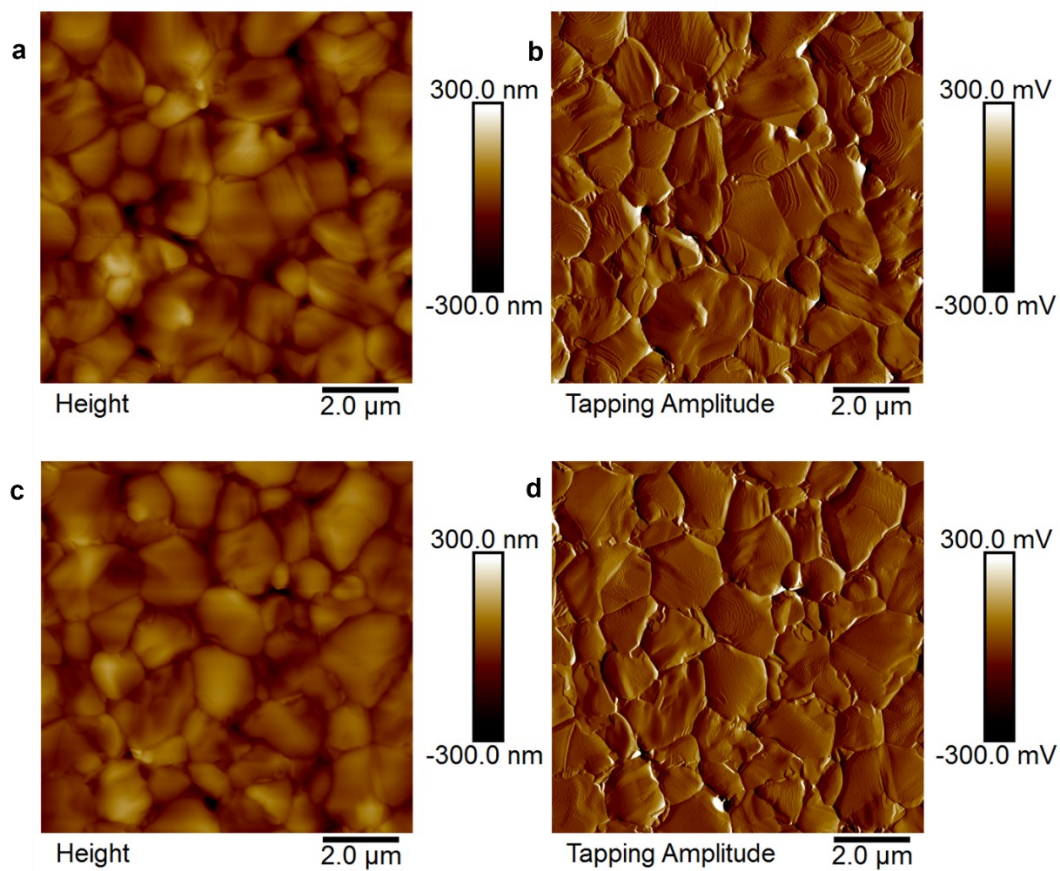


Fig. S7. (a) AFM image and (b) the corresponding tapping amplitude of the control perovskite film. (c) AFM image and (d) the corresponding tapping amplitude of the APC-treated perovskite film.

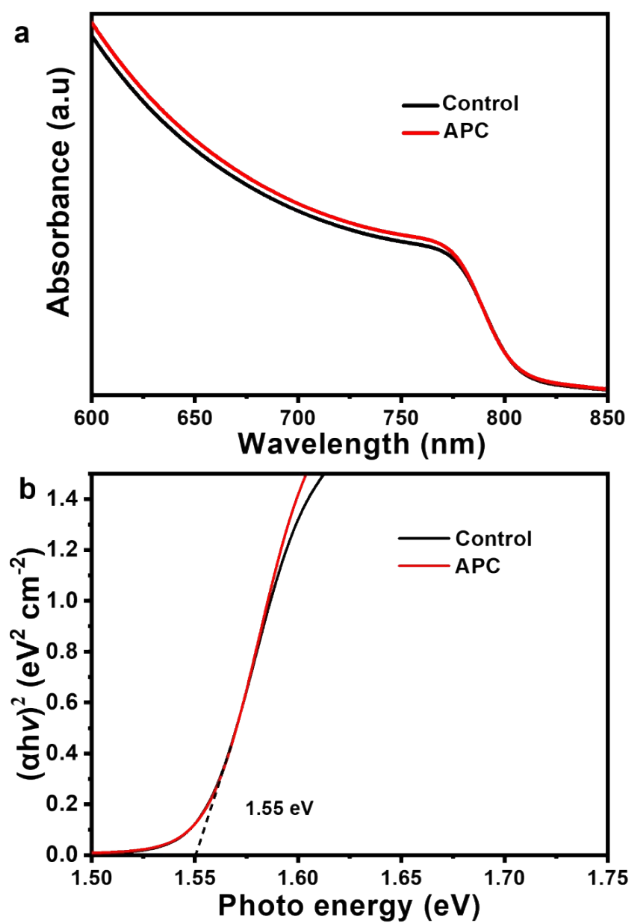


Fig. S8. (a) UV-vis absorption spectra of the control and APC treated perovskite films, (b) the corresponding bandgaps (1.55 eV).

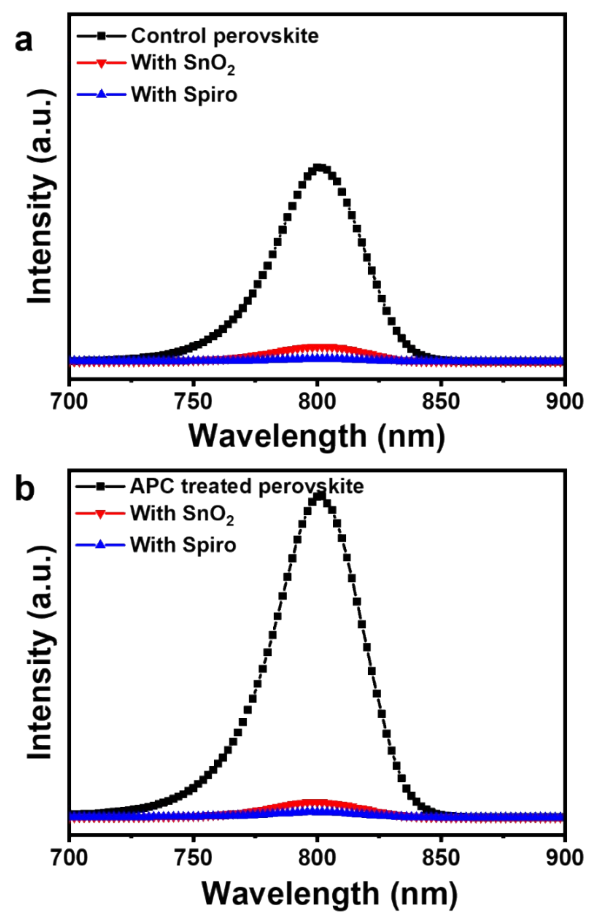


Fig. S9. PL spectra of control (a) and APC treated perovskite films (b) with SnO₂ and Spiro quenching layer, respectively.

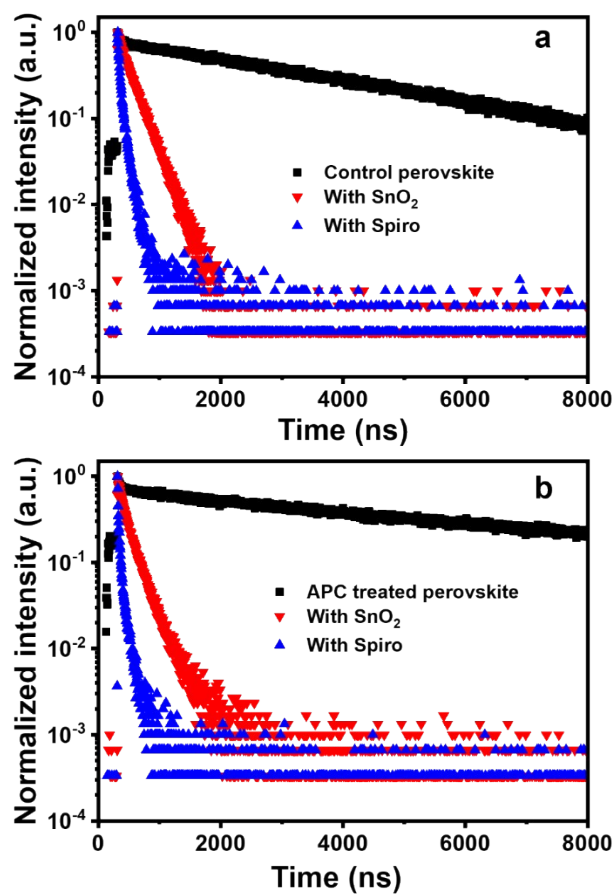


Fig. S10. TRPL spectra of control (a) and APC treated perovskite films (b) with SnO₂ and Spiro quenching layer, respectively.

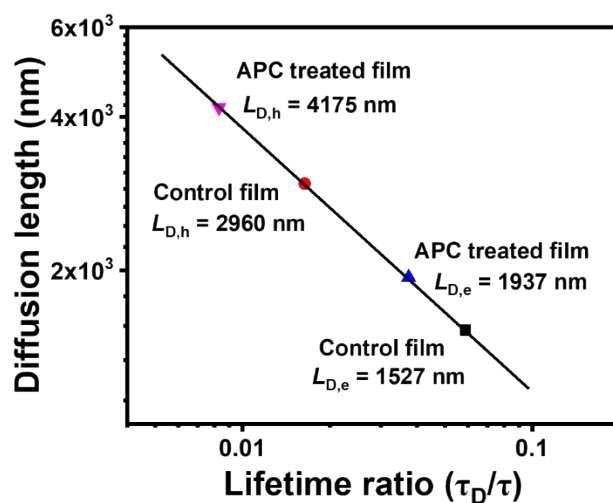


Fig. S11. The charge-carrier diffusion length of the control and APC treated perovskite films.

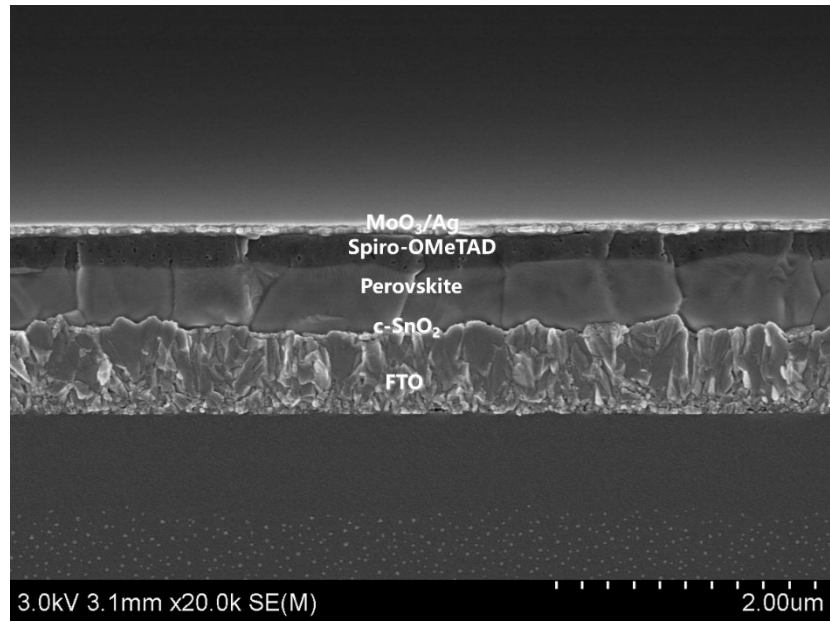


Fig. S12. Typical cross-sectional SEM image of the PSCs.

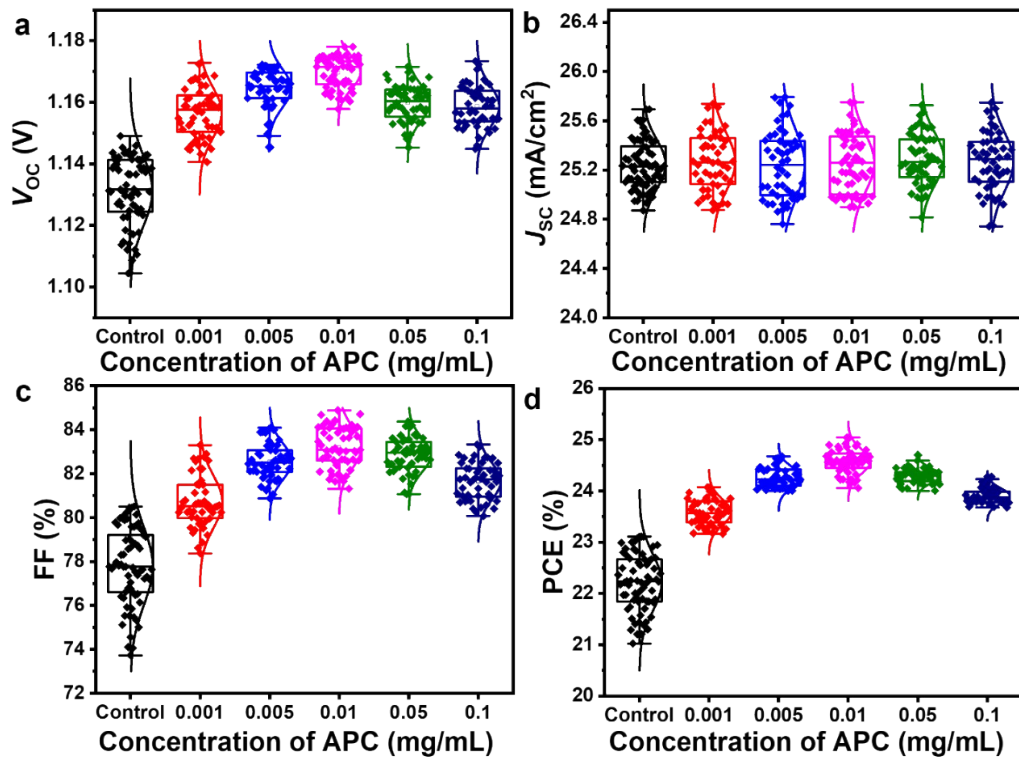


Fig. S13. Performance distribution of the devices with different APC concentrations (60 devices for each concentration).

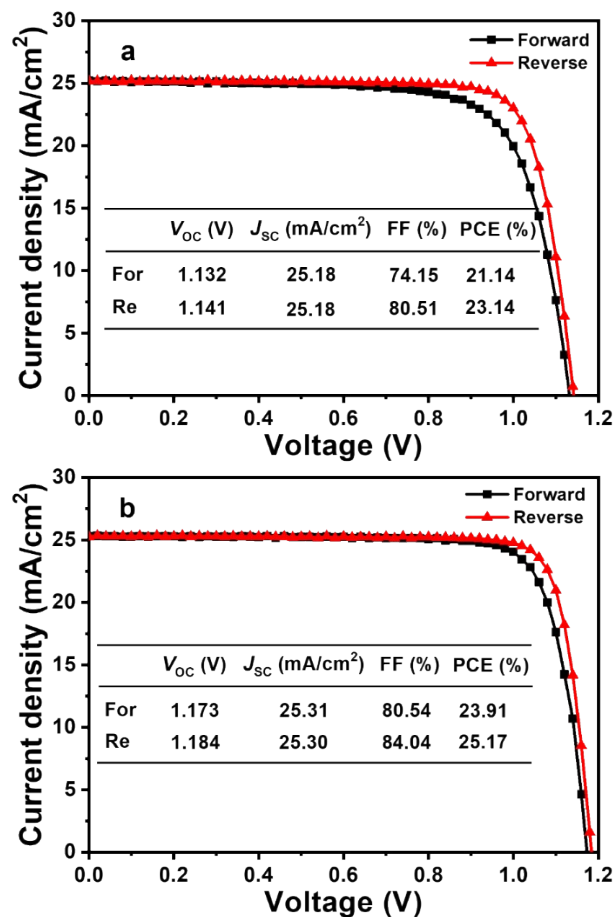


Fig. S14. Hysteretic effect of the champion devices based on the control (a) and APC treated perovskite films (b).

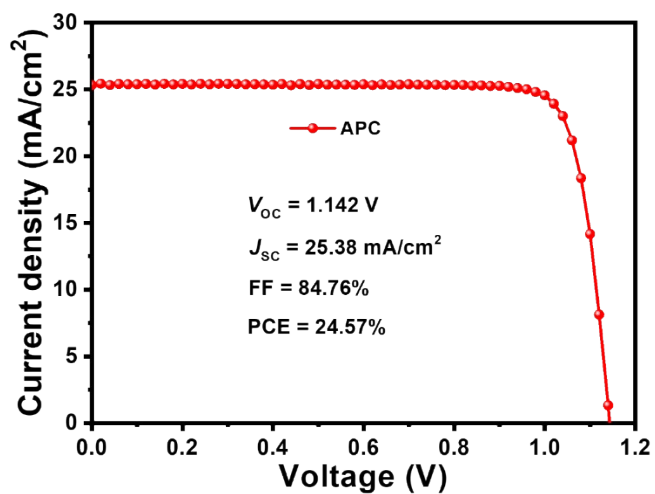


Fig. S15. J - V curve of APC treated PSC with an FF of 84.76%.



Fig. S16. The first page of certification report of photovoltaic performance of the APC treated perovskite solar cell from Chengdu Institute of Product Quality Inspection Co., Ltd.

Chengdu Institute of Product Quality Inspection Co., Ltd.
National Photovoltaic Product Quality Inspection & Testing Center
TEST REPORT

Test Report No. AGXB122W00240

Page 1 of 3

Product Name	APC treated perovskite solar cell	Trade Mark	/
Manufacture Date	13/06/2022	Model /Type	9.0 mm ²
Sample No.	AGXB122W00240	Sample Grade	/
Sample Quantity	One piece	Sample State	Normal
Delivery Date	13/06/2022	Sample Delivered personnel	Qiang Peng
Commission unit	Sichuan University	Manufacturer	Sichuan University
Commission unit address	No.24 South Section 1, Yihuan Road, Chengdu, Sichuan, P. R.	Manufacturer Address	No.24 South Section 1, Yihuan Road, Chengdu, Sichuan, P. R.
Commission unit Zip code	610065	Manufacturer Zip code	610065
Commission unit Tel.	15828019886	Manufacturer Tel.	15828019886
Center Address	No. 355, 2 nd Tengfei Road, Southwest Airport Economic Development Zone, Chengdu, Sichuan, P. R. China.	Measurement Date	14/06/2022
Methods	IEC60904-1:2006 Photovoltaic devices-Part 1: Measurement of Photovoltaic Current-Voltage Characteristics.		
Test conclusion	This column blank.		
Remarks	Original sample No. 1 , Cell area : 9.0 mm ² .		
Approved by	夏庆培	Reviewed by	成皓楠
		Measured by	张维



Fig. S17. The second page (sample information, test methods and cell area) of certification report of photovoltaic performance of the APC treated perovskite solar cell from Chengdu Institute of Product Quality Inspection Co., Ltd.

Chengdu Institute of Product Quality Inspection Co., Ltd.
National Photovoltaic Product Quality Inspection & Testing Center
TEST REPORT

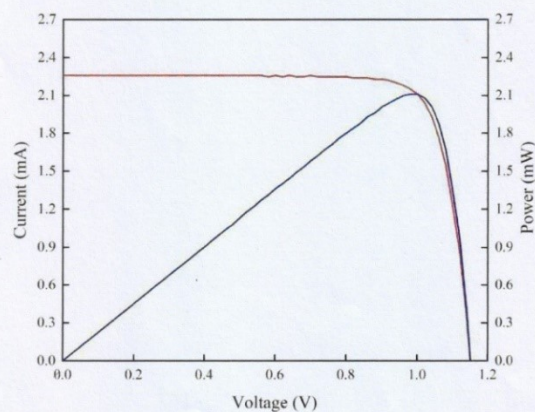
Test Report No. AGXB122W00240

Page 2 of 3

Test Results (Forward scanning) :

No.	Test item(s)	Unit	Results
1	Current-voltage characteristics measurement	---	---
1.1	Open-circuit voltage, V_{oc}	V	1.151
1.2	Short-circuit current, I_{sc}	mA	2.261
1.3	Maximum-power, P_{max}	mW	2.109
1.4	Maximum-power voltage, V_{p-max}	V	1.000
1.5	Maximum-power current, I_{p-max}	mA	2.109
1.6	Fill factor, FF	%	81.04
1.7	Conversion efficiency, η	%	23.43

Current-voltage characteristics under STC



Remark: Sample was tested under the irradiation with a steady-state class calibrated AAA solar simulator (AM1.5-G 1000.0 W/m²) at 25.0 °C. Designated area defined by thin metal aperture mask.

Fig. S18. J - V curves and photovoltaic parameters of the APC treated perovskite solar cell in forward scan from Chengdu Institute of Product Quality Inspection Co., Ltd.

Chengdu Institute of Product Quality Inspection Co., Ltd.
National Photovoltaic Product Quality Inspection & Testing Center
TEST REPORT

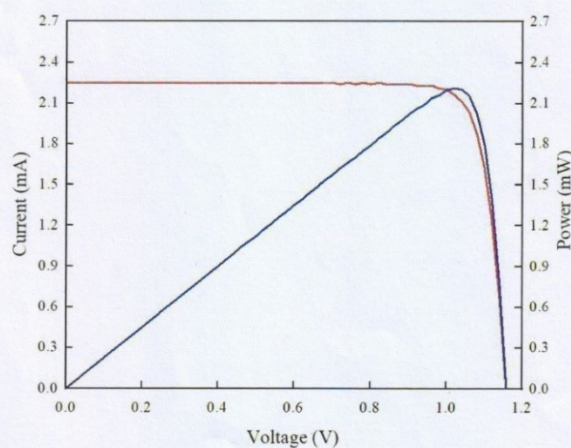
Test Report No. AGXB122W00240

Page 3 of 3

Test Results (Reverse scanning) :

No.	Test item(s)	Unit	Results
1	Current-voltage characteristics measurement	---	---
1.1	Open-circuit voltage, V_{OC}	V	1.158
1.2	Short-circuit current, I_{SC}	mA	2.251
1.3	Maximum-power, P_{max}	mW	2.206
1.4	Maximum-power voltage, V_{p-max}	V	1.020
1.5	Maximum-power current, I_{p-max}	mA	2.163
1.6	Fill factor, FF	%	84.64
1.7	Conversion efficiency, η	%	24.51

Current-voltage characteristics under STC



Remark: Sample was tested under the irradiation with a steady-state class calibrated AAA solar simulator (AM1.5-G 1000.0 W/m²) at 25.0 °C. Designated area defined by thin metal aperture mask.

Blank

Fig. S19. *J-V* curves and photovoltaic parameters of the APC treated perovskite solar cell in reverse scan from Chengdu Institute of Product Quality Inspection Co., Ltd.

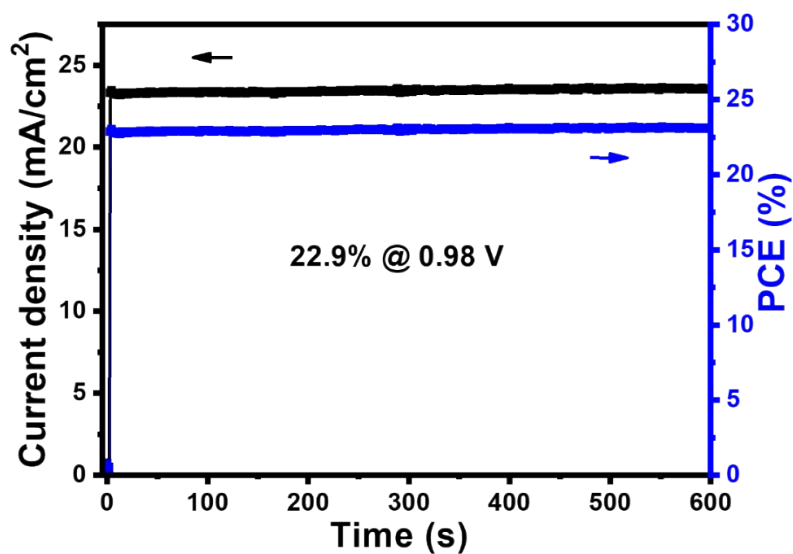


Fig. S20. Stabilized output efficiency of the control device around the maximum output power point as a function of time under simulated 1 sun illumination.

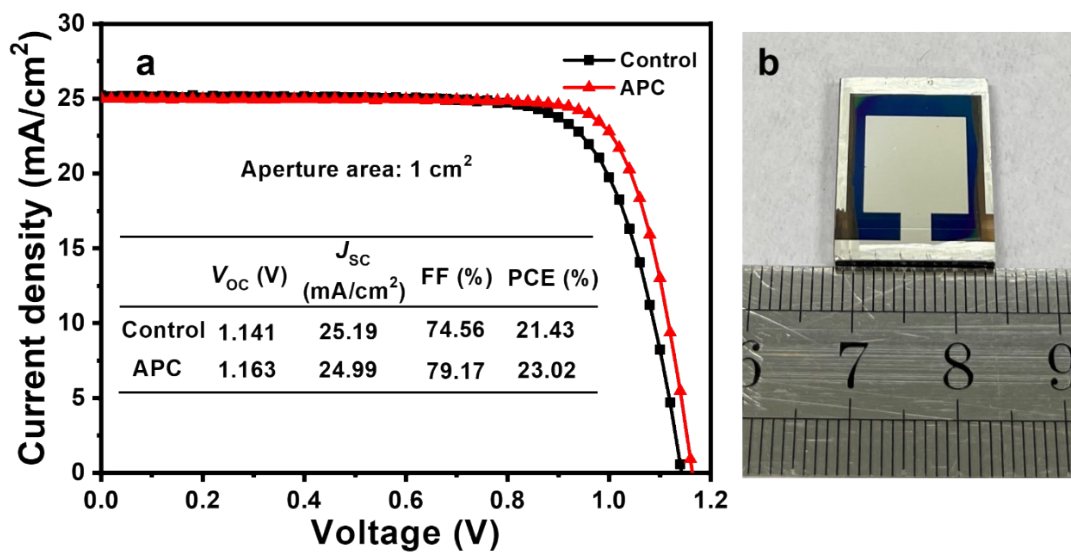


Fig. S21. (a) J - V curves of the large area (aperture area: 1 cm²) FAMA-based PSCs with and without APC-treatment. (b) The photograph of the large area PSCs.

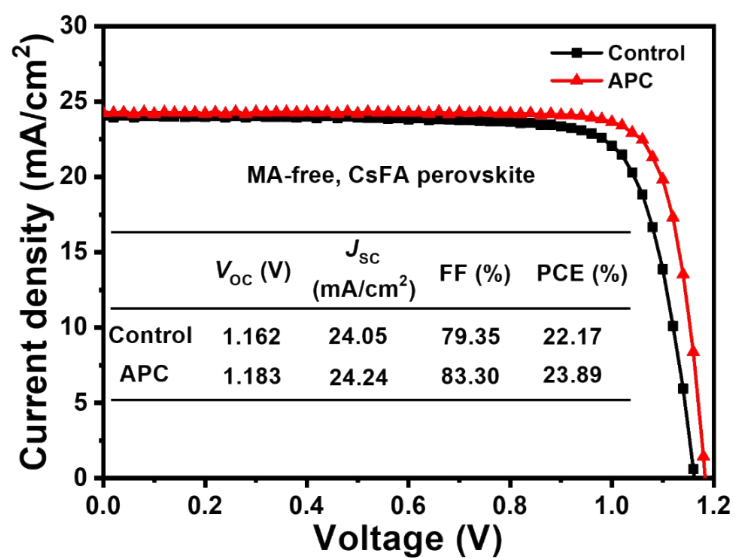


Fig. S22. J - V curves of the MA-free, CsFA-based PSCs (aperture area: 0.09 cm²) with and without APC-treatment.

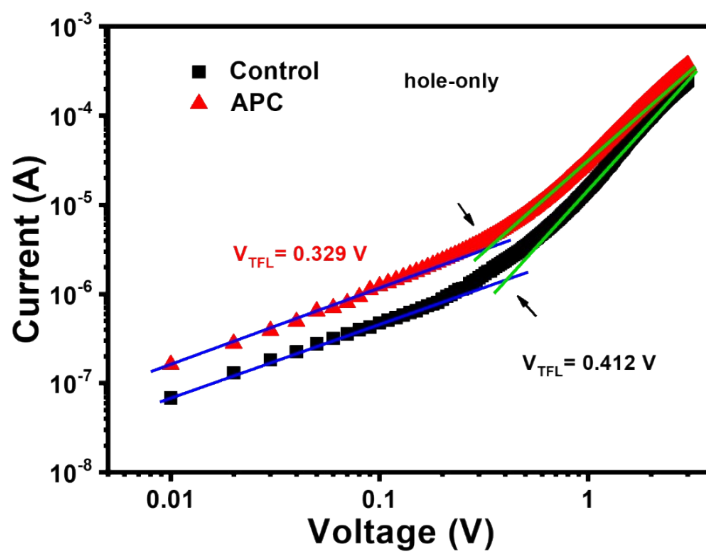


Fig. S23. Dark current-voltage curves for the hole-only structured devices with control and APC treated perovskites (FTO/PEDOT:PSS/Perovskite/Spiro/Au).

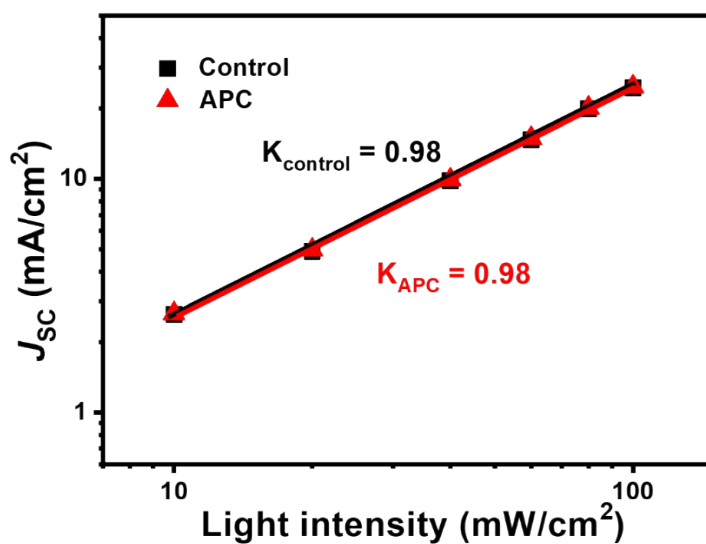


Fig. S24. J_{SC} vs. light intensity for the devices without and with APC treatment.

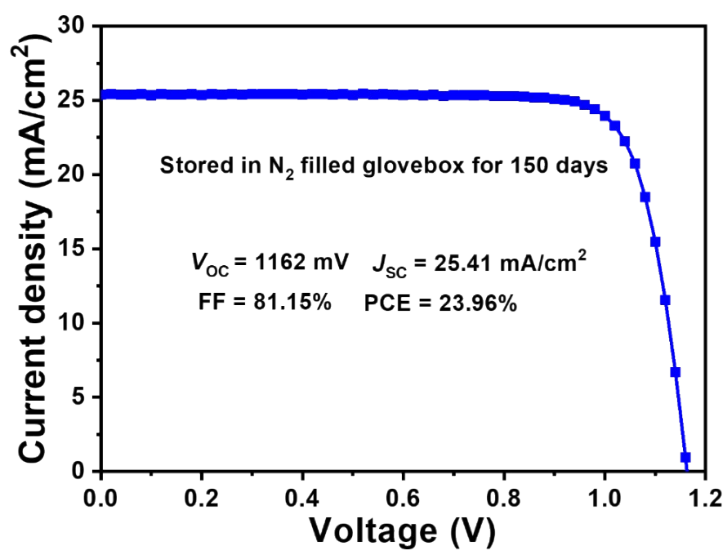


Fig. S25. J - V curve of the APC treated device after storing at a N₂-filled glovebox for 150 days.

Table S1. Parameters of the TRPL spectroscopy based on different samples.

Samples	τ_{ave} (ns)	τ_1 (ns)	τ_2 (ns)	A_1	A_2
Glass/Control perovskite	3798.53	22.35	3803.59	0.18	0.79
Glass/FTO/SnO ₂ /Control perovskite	223.73	40.87	230.07	0.16	0.82
Glass/Control perovskite/Spiro	62.27	16.70	75.75	0.55	0.41
Glass/APC treated perovskite	4930.65	47.33	4950.55	0.26	0.61
Glass/FTO/SnO ₂ /APC treated perovskite	184.75	45.35	200.99	0.32	0.62
Glass/APC treated perovskite/Spiro	40.93	9.21	54.71	0.72	0.28

Table S2. PV parameters of 60 control devices.

Entry	V_{OC} (V)	J_{SC} (mA cm ⁻²)	FF (%)	PCE (%)
1	1.143	25.61	73.72	21.57
2	1.144	24.87	76.76	21.84
3	1.141	25.19	74.56	21.43
4	1.137	25.00	77.04	21.89
5	1.137	25.12	76.79	21.92
6	1.144	25.15	76.60	22.03
7	1.144	25.39	76.62	22.25
8	1.130	25.00	78.64	22.21
9	1.129	25.35	75.84	21.71
10	1.143	25.49	77.35	22.55
11	1.133	25.24	76.48	21.88
12	1.146	25.38	77.72	22.61
13	1.125	25.44	74.11	21.20
14	1.117	25.13	75.54	21.21
15	1.114	25.46	75.47	21.40
16	1.117	25.08	76.34	21.39
17	1.112	25.26	77.76	21.85
18	1.105	25.12	77.52	21.51
19	1.112	25.26	77.76	21.85
20	1.127	24.93	77.38	21.74

21	1.123	25.29	74.06	21.02
22	1.126	25.19	75.92	21.54
23	1.132	25.45	75.33	21.69
24	1.130	25.33	79.58	22.77
25	1.131	25.55	79.02	22.83
26	1.118	25.46	79.58	22.66
27	1.137	25.60	78.57	22.87
28	1.111	25.69	76.52	21.83
29	1.124	25.44	78.87	22.56
30	1.104	25.59	77.86	22.00
31	1.131	25.09	75.53	21.43
32	1.130	25.23	77.54	22.11
33	1.115	25.34	77.81	21.98
34	1.132	25.42	79.94	23.00
35	1.139	24.95	78.96	22.44
36	1.138	24.98	79.65	22.64
37	1.138	24.95	79.89	22.68
38	1.145	25.07	80.46	23.11
39	1.140	25.23	78.81	22.66
40	1.123	25.11	77.63	21.89
41	1.118	25.46	77.97	22.19
42	1.139	25.03	79.75	22.72
43	1.141	25.13	80.45	23.07
44	1.140	24.98	80.51	22.92
45	1.149	25.15	79.97	23.11
46	1.124	25.61	79.47	22.88
47	1.141	25.23	79.98	23.03
48	1.126	25.44	79.21	22.70
49	1.142	25.23	77.22	22.25
50	1.137	25.69	76.40	22.32
51	1.141	25.51	78.32	22.80
52	1.125	25.02	78.72	22.16
53	1.141	25.25	79.67	22.95
54	1.139	25.13	77.82	22.27
55	1.138	25.28	77.31	22.24
56	1.128	25.16	75.01	21.29
57	1.131	25.10	77.68	22.05
58	1.131	25.07	75.12	21.30

59	1.142	25.20	77.21	22.21
60	1.143	25.61	73.72	21.57
Average	1.131±0.01	25.26±0.21	77.55±1.80	22.16±0.57

Table S3. PV parameters of 60 APC treated devices.

Entry	V_{OC} (V)	J_{SC} (mA cm ⁻²)	FF (%)	PCE (%)
1	1.174	24.98	84.06	24.64
2	1.176	25.00	84.55	24.86
3	1.175	25.38	82.97	24.74
4	1.171	25.44	84.04	25.03
5	1.173	24.99	83.05	24.35
6	1.161	25.16	83.87	24.50
7	1.166	25.57	83.61	24.93
8	1.163	25.51	84.42	25.04
9	1.170	25.49	82.39	24.58
10	1.172	25.40	82.65	24.60
11	1.175	25.31	83.15	24.72
12	1.178	25.51	81.88	24.61
13	1.175	25.51	81.94	24.56
14	1.167	24.97	84.09	24.50
15	1.161	25.18	84.24	24.62
16	1.175	25.13	83.03	24.52
17	1.172	24.96	82.61	24.18
18	1.172	25.60	81.66	24.49
19	1.175	24.95	82.64	24.22
20	1.173	25.52	83.08	24.88
21	1.166	25.44	83.64	24.81
22	1.171	25.41	82.12	24.44
23	1.172	25.75	82.56	24.91
24	1.166	25.75	82.79	24.87
25	1.169	25.09	83.63	24.52
26	1.173	25.28	81.65	24.21
27	1.171	25.18	82.16	24.21
28	1.166	24.99	83.90	24.45
29	1.173	25.24	83.05	24.59
30	1.178	25.51	81.88	24.61

31	1.175	25.51	81.94	24.56
32	1.175	25.17	82.76	24.47
33	1.175	25.29	81.32	24.16
34	1.174	24.98	84.06	24.64
35	1.175	24.95	82.64	24.22
36	1.173	25.29	82.68	24.54
37	1.175	25.18	82.97	24.55
38	1.175	24.93	83.03	24.32
39	1.164	25.65	82.09	24.50
40	1.167	25.14	84.09	24.67
41	1.162	25.31	84.21	24.76
42	1.161	25.40	83.86	24.74
43	1.167	24.98	84.39	24.60
44	1.167	25.27	84.09	24.79
45	1.163	24.90	84.24	24.39
46	1.160	25.51	84.13	24.90
47	1.158	25.11	84.68	24.61
48	1.165	25.38	84.71	25.05
49	1.164	25.08	84.12	24.57
50	1.163	25.26	83.70	24.58
51	1.163	24.98	83.29	24.20
52	1.169	25.00	83.08	24.27
53	1.174	25.20	83.46	24.68
54	1.172	25.47	82.60	24.66
55	1.172	25.12	81.74	24.05
56	1.171	24.99	82.12	24.03
57	1.145	25.79	83.54	24.68
58	1.166	25.44	82.69	24.52
59	1.166	24.76	83.89	24.22
60	1.161	25.09	82.45	24.03
Average	1.169±0.01	25.26±0.24	83.16±0.89	24.55±0.25

Table S4. EIS parameters of the devices based on the control and APC treated perovskite films.

Devices	R_{tr} (Ω)	CPE1 (F)	R_{rec} (Ω)	CPE2 (F)
Control	28502	14.03E-9	3.63E6	0.77E-6

APC

22540

40.06E-9

5.70E6

1.16E-6

Table S5. Time evolution of the PV parameters for PSCs with and without APC treatment.

Devices	Time (days)	V_{OC} (V)	J_{SC} (mA cm ⁻²)	FF (%)	PCE (%)	
Control	0	1.139	25.29	80.25	23.11	
	7	1.141	25.24	80.04	23.05	
	14	1.141	25.25	79.67	22.95	
	21	1.140	25.23	78.81	22.66	
	28	1.143	25.23	77.63	22.39	
	35	1.142	25.23	77.22	22.25	
	42	1.131	25.16	77.23	21.97	
	60	1.138	25.15	76.38	21.86	
	90	1.129	25.35	75.84	21.71	
	120	1.131	25.29	75.69	21.65	
	150	1.114	25.46	75.47	21.40	
	APC treated perovskite	0	1.171	25.44	84.04	25.03
		7	1.165	25.38	84.71	25.04
		14	1.166	25.57	83.61	24.92
21		1.166	25.44	83.64	24.81	
28		1.162	25.31	84.21	24.75	
35		1.161	25.18	84.24	24.63	
42		1.169	25.09	83.63	24.53	
60		1.166	25.44	82.69	24.52	
90		1.171	25.41	82.12	24.44	
120		1.171	25.18	82.16	24.22	
150		1.162	25.41	81.15	23.96	